Received: 16 January 2020 | Revised: 17 March 2020 | Accepted: 31 May 2020

DOI: 10.1002/mmce.22342

RESEARCH ARTICLE

INTERNATIONAL JOURNAL OF RF AND MICROWAVE COMPUTER-AIDED ENGINEERING WILEY

A testbench of arbitrary accuracy for electromagnetic simulations

Adrian Amor-Martin

Lehrstuhl für Theoretische Elektrotechnik, Universität des Saarlandes, Saarbrücken, Saarland, Germany

Correspondence
Adrian Amor-Martin, Lehrstuhl für Theoretische Elektrotechnik, Universität des Saarlandes, Campus C6.3, 11.OG, Saarbrücken, Germany.
Email: aamor89@gmail.com

Abstract

Several electromagnetic problems for verification purposes in computational electromagnetics are introduced. Details about the formulation of a generalized eigenvalue problem for non-lossy and lossy materials are provided to obtain a fast and ready-to-use way of verification. Codes written using the symbolic toolbox from MATLAB are detailed to obtain an arbitrary accuracy for the proposed problems. Finally, numerical results in a finite element method code are presented together with the analytical values to show the accuracy of the code proposed.

KEYWORDS

basis functions, finite element method, testbench, validation, verification

1 | INTRODUCTION

In the last years, the capabilities of computational resources have increased almost exponentially. The field of computational electromagnetics (CEM) have also benefited from this trend, solving large problems which were unreachable a few years before.[1,2]

It is strongly advised that a testbench for automatic testing is available with the development of new code features, for example, Reference 3. For example, in the context of the finite element method (FEM), small changes in the assembly strategy,[4,5] in the integration rules,[6] in the use of universal matrices to perform the assembly,[7] or in the use of different shapes (tetrahedra,[8] triangular prisms,[9] hexahedra,[10] or even pyramids,[11]) may introduce small numerical errors which might not be detected in real-life applications, where the requested accuracy is not so high. This testbench can also be used for using new finite element suites in electromagnetics.[12,13] These suites have a wide range of applications and running a testbench to assess their performance is advisable. Finally, new approaches such as serendipity space of functions,[14] or isogeometric basis functions,[15] could also benefit from a standard testbench.

The intensive research in FEM for electromagnetics in the 90s provided with a number of cavity problems that can be used for testing an electromagnetic code.[16,17] These problems may be used for different methods as well,[18,19] and are a good starting point to test, for example, a FEM code since only stiffness and mass matrices need to be constructed. The solution may be obtained with the application of an eigenvalue solver, for example, Reference 20. However, when these problems were formulated, high accuracy was not necessary due to computational limitations. Thus, it is hard to find expressions and analytical values ready to use for the FEM practitioner, which is critical when using high order basis functions where high accuracies are obtained with a relatively small number of unknowns: now, accuracies close to the machine precision are achievable with good code practices in a personal laptop. To obtain arbitrary accuracy for the analytic solution, many commercial symbolic mathematical tools are readily available.[21,22] Here, the symbolic toolbox of MATLAB,[23] based on MuPAD,[24] is used.

In this communication, a set of eigenvalue problems which can be used to test electromagnetic codes is proposed. Specifically, four tests are suggested: first, a rectangular cavity which is the most straightforward test for stiffness and mass matrices; second, a half-filled cavity which introduces a problem with two different materials; third, a lossy half-filled cavity which tests a basic formulation with losses; and finally, a circular cavity which introduces curved elements in the equation. These tests are not randomly chosen: the first test is one of the most used in the literature due to the easiness of its formulation. The second one, which requires a transcendental equation to be solved, tests the use of different materials in the equation. The third test shows one possible way to introduce losses in electromagnetic simulations, and it is easy to use since the same transcendental equation (but with losses) needs to be solved. Finally, the fourth problem is a circular cavity which is easy to formulate but Bessel functions might introduce some problems with arbitrary resolution.[25] Note that these eigenvalue problems have already been tested in the community, but as far as the author knows, the solution with arbitrary accuracy has not been made public. As already commented, to use analytical results with a single-precision accuracy was enough some years ago; however, with the use of higher-order basis functions being more and more frequent due to the new computational capabilities (eg, References 8 and 11), more accurate results are mandatory. Thus, the goal of this paper is to save time for CEM practitioners with the availability of these results.

The paper is structured as follows: in Section 2, a possible formulation to solve these cavities is detailed; in Section 3, the derivation of the analytical results and codes to obtain them with arbitrary accuracy are provided; in Section 4, the analytical values for the dominant modes and numerical results using a FEM code are presented; finally, in Section 5, conclusions from this paper are drawn.

2 | FORMULATION

A double curl-wave equation may be used to determine the boundary value problem in a given domain Ω through

$$\nabla\times\mu_r^{-1}(\nabla\times\boldsymbol{E})-k_0^2\varepsilon_r\boldsymbol{E}=\mathbf{0} \tag{1}$$

where μ_r and ε_r are the magnetic permeability and electric permittivity of the material respectively, E is the electric field and k_0 stands for the wavenumber. To close the domain, a Dirichlet boundary condition is set on the walls of the cavity $\partial\Omega$ with

$$\hat{\boldsymbol{n}}\times\boldsymbol{E}=\mathbf{0}\text{ on }\partial\Omega. \tag{2}$$

If a FEM problem is used to solve this problem, after the application of the Galerkin method the following variational formulation may be obtained,

$$\left(\nabla\times\mathbf{w},\mu_r^{-1}\nabla\times\boldsymbol{E}\right)_\Omega-k_0^2(\mathbf{w},\varepsilon_r\boldsymbol{E})_\Omega=\mathbf{0}, \tag{3}$$

where $\boldsymbol{w}$ is the test function belonging to the same space as the electric field, that is,[26]

$$\boldsymbol{H}(\text{curl},\Omega):=\left\{\boldsymbol{w}\in[L_2(\Omega)]^3\,|\,\nabla\times\boldsymbol{w}\in[L_2(\Omega)]^3\right\}, \tag{4}$$

with $L_2(\Omega)$ as the space of square-integrable functions over Ω. Inner products $(\boldsymbol{w},\boldsymbol{x})$ are defined on a domain Ω as

$$(\boldsymbol{w},\boldsymbol{x})_\Omega=\int_\Omega\boldsymbol{w}\cdot\boldsymbol{x}\,d\Omega \tag{5}$$

Note that an equivalent formulation with the magnetic field $\boldsymbol{H}$ may also be used.

The discretization of this problem leads to the following matrix equation,

$$\left(\boldsymbol{K}-k_0^2\boldsymbol{M}\right)\boldsymbol{v}=0, \tag{6}$$

which corresponds to a generalized eigenvalue problem with k_0^2 and $\boldsymbol{v}$ as eigenvalues and eigenvectors, respectively. The matrices $\boldsymbol{K}$ and $\boldsymbol{M}$ are the so-called stiffness and mass matrices (for FEM practitioners), which can be defined elementwise with

$$M_{\text{ij}}=\left(\boldsymbol{w}_j,\varepsilon_r\boldsymbol{w}_j\right), \tag{7}$$

$$K_{\text{ij}}=\left(\nabla\times\boldsymbol{w}_i,\mu_r^{-1}\nabla\times\boldsymbol{w}_j\right). \tag{8}$$

This formulation is valid to get the cutoff frequency of the different modes for the rectangular, half-filled, and circular cavities. However, for the lossy cavity, an additional step into the formulation might be introduced (see, eg, Reference 19). Now, a modified electric permittivity ε_r' is used,

$$\varepsilon_r'=\varepsilon_r-j\frac{\sigma\eta_0}{k_0}, \tag{9}$$

where η_0 is the characteristic impedance of vacuum, σ is the conductivity of the material, and j is the imaginary unit. From Equation (10), and with $\nu=jk_0$,

$$\left(\boldsymbol{K}+\left(\nu^2+\nu\frac{\sigma\eta_0}{\varepsilon_r}\right)\boldsymbol{M}\right)\boldsymbol{v}=\boldsymbol{0}, \tag{10}$$

and unfolding $\boldsymbol{v}$ into $\boldsymbol{v_1}$ and $\boldsymbol{v_2}=\boldsymbol{v_1}$,

$$\begin{pmatrix}\boldsymbol{K} & 0\\ 0 & I\end{pmatrix}\begin{pmatrix}\boldsymbol{v}_1\\ \boldsymbol{v}_2\end{pmatrix}=\nu\begin{pmatrix}-\frac{\sigma\eta_0}{\varepsilon_r}\boldsymbol{M} & -\boldsymbol{M}\\ I & 0\end{pmatrix}\begin{pmatrix}\boldsymbol{v}_1\\ \boldsymbol{v}_2\end{pmatrix} \tag{11}$$

follows, where I corresponds to the identity matrix.

3 | ANALYTICAL RESULTS WITH ARBITRARY ACCURACY

Here, the analytical results are shown first and, then, the code in MATLAB is provided.

3.1 | Rectangular cavity

This cavity is a good starting point since it is the most straightforward problem that can be solved. The analytical wavenumber may be obtained by,[27]

$$k_{0,\text{anal}}^2=\left(\frac{m\pi}{a}\right)^2+\left(\frac{n\pi}{b}\right)^2+\left(\frac{p\pi}{c}\right)^2,\forall\begin{cases}p>0,m,n\geq 0\\ p\geq 0,m,n>0\end{cases} \tag{12}$$

where the first line of constraints refer to the transversal electric (TE) modes, and the second line of constraints apply to the transversal magnetic (TM) modes. Geometrical parameters a, b and c are shown in Figure 1. To get results with arbitrary accuracy, MATLAB code shown in Figure 2 is used. Note that the use of the symbolic package is mandatory to use the functions *vpa* and *digits*. Also, in order not to affect other parts of the code which execute that function, the variable *digitsOld* is used to restore the previous resolution. The output variable indices allow identifying the mode of a given k_0, showing in the fourth index if it corresponds to a TE mode (−1) or a TM mode (−2).

3.2 | Half-filled cavity

To obtain the analytical result, the analysis for partially filled waveguides from Reference 27 is followed. Geometrical parameters and layout are shown in Figure 1. The potential functions for the TE^z components are, for the dielectric region

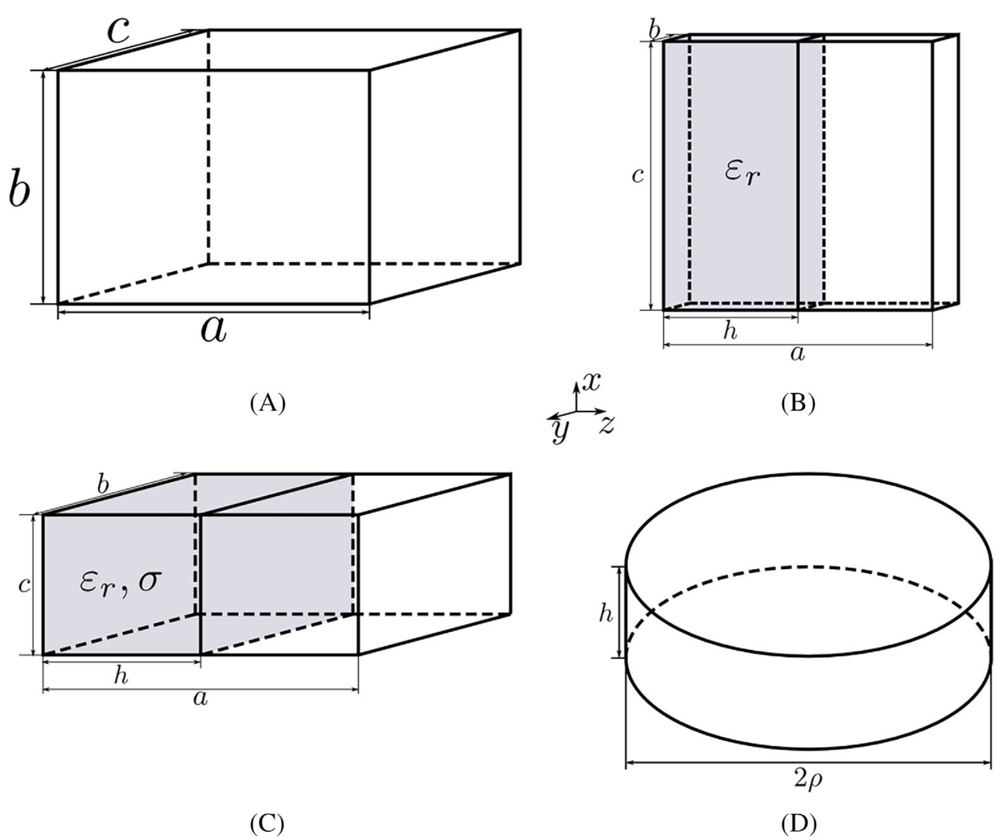

FIGURE 1 The four cavities solved in Section 3: A, Rectangular cavity; B, Half-filled cavity; C, Lossy cavity; D, Circular cavity

```
function [ kc , indices ]=getAllKcFromRectCavity(a ,b, c ,numKc, resolution )

  % Default resolution
  if (nargin == 4)
    resolution = 16;
  end
  % Change the resolution of  the symbolic package.
  digitsOld = digits (resolution);
  kc = sym(zeros(1, 2*(numKc+1)^3));
  indices = zeros (4 , 2*(numKc+1)^3);

  counter = 1;

  for m = 0:numKc
      for n = 0:numKc
        if    ((m==0)     &&     (n==0))
          continue
        end
     for p = 0:numKc
        if (p>0)  % TE mode
                   kc (counter) = sqrt ((m*pi/a)^2+(n*pi/b)^2+(p*pi/c )^2);
                   indices (:,counter) = [m, n, p, −1];
                   counter = counter + 1;
        end
        if ((m>0) && (n>0))  % TM mode
                   kc( counter ) = sqrt ((m*pi/a)^2+(n*pi/b)^2+(p*pi/c )^2);
                   indices (: , counter ) = [m, n, p, −2];
                   counter = counter + 1;
         end
     end
   end
 end  % To remove zeros .

  indices = indices (: ,1: counter −1);
  kc = vpa(kc (:,1:counter −1), resolution);

  [kc, sortedIndices] = sort(kc);

  indices = indices (:, sortedIndices );

  kc = kc (1:numKc);

  indices = indices (: ,1:numKc);

 % Restore         previous         resolution.
  digits ( digitsOld )
```

FIGURE 2 Code used in Section 3.1

$$F_z^d(x,y,0\geq z\geq h) = A_{\mathrm{mn}}^d\cos(\beta_{\mathrm{xd}}x)\sin(\beta_{\mathrm{zd}}z)\times \left[C_3^d\cos\left(\beta_{\mathrm{yd}}y\right)+D_3^d\sin\left(\beta_{\mathrm{yd}}y\right)\right], \tag{13}$$

while for the remaining part of the cavity,

$$F_z^0(x,y,h\geq z\geq a) = A_{\mathrm{mn}}^0\cos(\beta_{x0}x)\sin(\beta_{z0}z)\times \left[C_3^0\cos(\beta_{y0}y)+D_3^0\sin(\beta_{y0}y)\right], \tag{14}$$

with

$$\begin{aligned} \beta_{xd} &= \beta_{x0} = \frac{m\pi}{c}, \forall m\geq 0 \\ \beta_d^2 &= \beta_{xd}^2+\beta_{yd}^2+\beta_{zd}^2 = \omega^2\mu_d\varepsilon_d, \\ \beta_0^2 &= \beta_{x0}^2+\beta_{y0}^2+\beta_{z0}^2 = \omega^2\mu_0\varepsilon_0, \end{aligned} \tag{15}$$

where ω is the angular frequency, β_i is the propagation constant in the i-th component and ε_d, μ_d are the electric permittivity and magnetic permeability of the dielectric material respectively. Additional boundary conditions must be imposed,

$$\begin{aligned} {E_x}^d(0\geq x\geq c, y=0, 0\geq z\geq h) &= 0, \\ {E_x}^d(0\geq x\geq c, y=b, 0\geq z\geq h) &= 0, \\ {E_x}^0(0\geq x\geq c, y=0, h\geq z\geq a) &= 0, \\ {E_x}^0(0\geq x\geq c, y=b, h\geq z\geq a) &= 0. \end{aligned} \tag{16}$$

Following a similar procedure as with rectangular cavities, it may be obtained that

$$D_3^0 = D_3^d$$
$$\beta_{yd} = \beta_{y0} = \frac{n\pi}{b}, \forall n \geq 0 \tag{17}$$

Thus, as with partially filled waveguides, a transcendental equation have to be solved which is

$$\frac{\beta_{z0}}{\mu_0}\cot[\beta_{z0}(b-h)] + \frac{\beta_{zd}}{\mu_d}\cot[\beta_{zd}h] = 0, \tag{18}$$

given that $\beta_{z0} = \beta_{zd} = k_{0,\text{ anal}}$. Using Equation (15) and considering that $\mu_d = \mu_0$,

$$\phi(1)\cot(\phi(1)(c-h)) = -\phi(\varepsilon_r)\cot(\phi(\varepsilon_r)h), \tag{19}$$

follows, with

$$\varphi(\varepsilon_r) = \sqrt{\varepsilon_r k_{0,\text{anal}}^2 - \left(\frac{m\pi}{a}\right)^2 - \left(\frac{n\pi}{b}\right)^2}. \tag{20}$$

Regarding TM^z modes, a similar analysis leads to

$$\frac{\beta_{z0}}{\varepsilon_0}\tan[\beta_{z0}(b-h)] + \frac{\beta_{zd}}{\varepsilon_d}\tan[\beta_{zd}h] = 0. \tag{21}$$

For TE modes, the couple $m = n = 0$ is forbidden, and for TM modes, $m \geq 1$, $n \geq 1$.

The MATLAB code shown in Figure 3 is used to obtain the results with arbitrary accuracy.

Note that there are two modes of operation. First, a suitable guess needs to be provided due to the infinity number of solutions. Invoking

```
getKcFromHalfFilledCavity(a,b,c,h,epr,1,0,true,[300,900])
```

returns the figure shown in Figure 4, where it may be seen that exist three solutions in the range of $k_0 = [300, 900]\text{m}^{-1}$: around $k_0 = 300\text{m}^{-1}$, $k_0 = 600\text{m}^{-1}$ and $k_0 = 800\text{m}^{-1}$. These modes correspond, respectively, to $\text{TE}^z{}_{101}$, $\text{TE}^z{}_{102}$, and $\text{TE}^z{}_{103}$. With that, now

```
getKcFromHalfFilledCavity(a,b,c,h,epr,1,0,true,300,32)
```

may be called to obtain k_0 for $\text{TE}^z{}_{101}$ with the desired accuracy (in the example, 32 significant digits).

3.3 | Lossy cavity

Now, the material used in Section 3.2 is changed for a lossy material with a finite conductivity σ. The analytical results obtained in Section 3.2 hold if ε_r' from (9) instead of ε_r is used. This leads to the code shown in Figure 5.

```
function kc=getKcFromHalfFilledCavity (a ,b, c ,h, epr , m, n, TEFlag, axisLimits,
  resolution)

 kc = 0;

  syms kcsquared kcsym
  if (TEFlag)
     lhsEquation = sqrt( kcsquared −(m∗pi/a)^2−(n∗pi/b )^2)∗...
          cot(sqrt( kcsquared −(m∗pi/a)^2−(n∗pi/b)^2)∗(c−h ));
       rhsEquation = −sqrt( epr∗kcsquared −(m∗pi/a)^2−(n∗pi/b )^2)∗...
         cot(sqrt( epr∗kcsquared −(m∗pi/a)^2−(n∗pi/b)^2)∗h );
  else
     lhsEquation = sqrt( kcsquared −(m∗pi/a)^2−(n∗pi/b )^2)∗...
          tan(sqrt( kcsquared −(m∗pi/a)^2−(n∗pi/b)^2)∗(c−h ));
       rhsEquation = −sqrt( epr∗kcsquared −(m∗pi/a)^2−(n∗pi/b )^2)∗... tan(sqrt(
          epr∗kcsquared −(m∗pi/a)^2−(n∗pi/b)^2)∗h );
  end

  if (nargin > 9)
     digitsOld = digits (resolution);
     equation = lhsEquation−rhsEquation == 0;
     kc = (sqrt(vpasolve (equation, kcsquared,    axisLimits .^2)));
      digits(digitsOld);
  else
     close all
      fplot (real(lhsEquation), axisLimits.^2)
      hold on
      fplot (real(rhsEquation), axisLimits.^2);
  end
```

FIGURE 3 Code used in Section 3.2

A similar procedure may be used to get estimates and obtain the full accuracy solutions.

3.4 | Circular cavity

The analytical values for the wavenumber in TE modes are,[27]

$$k_{0,\mathrm{anal}}^2 = \left(\frac{\chi'_{mn}}{\rho}\right)^2 + \left(\frac{p\pi}{h}\right)^2, \forall m \geq 0, n, p > 0 \tag{22}$$

where χ'_{mn} represents the n-th zero of the derivative of the Bessel function J_m of the first kind of order m. For TM modes,

$$k_{0,\mathrm{anal}}^2 = \left(\frac{\chi_{mn}}{\rho}\right)^2 + \left(\frac{p\pi}{h}\right)^2, \forall m, p \geq 0, n > 0 \tag{23}$$

where χ_{mn} stands for the nth zero of the Bessel function J_m of the first kind of order m. Similarly to Section 3.1, a code as in Figure 6 may be written. The most intrincated aspect to take into account to obtain an arbitrary accuracy for this cavity is in the computation of χ_{mn} and χ'_{mn}. Indeed, in Reference 25, a detailed review of all the inaccuracies that may occur in this computation with a number of different mathematical libraries is shown. However, with reasonable guesses, the MATLAB code written in Figure 7 has proven to be accurate. This code uses only standard libraries from the symbolic package of MATLAB. The function getGuess returns the solution with an accuracy of two digits widely present in the literature (see, eg, Reference 27).

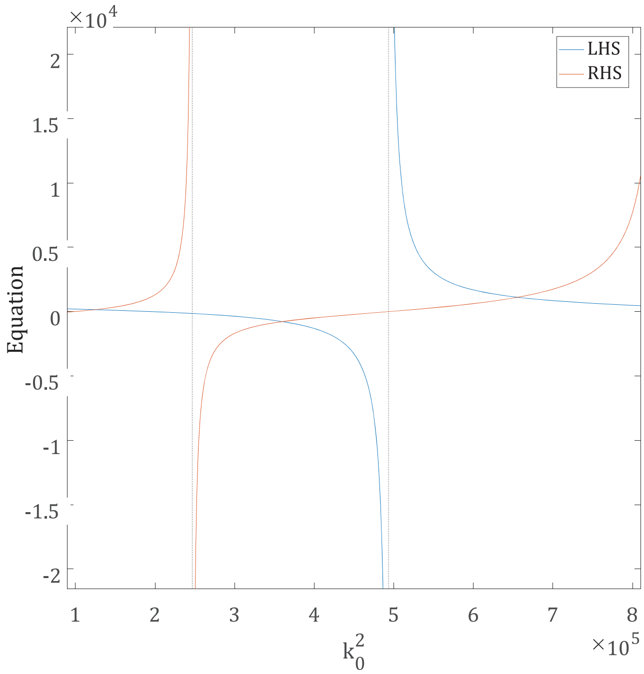

FIGURE 4 Solution for the range $k_0 = [300, 900]$ for Equation (19)

4 | NUMERICAL RESULTS

To justify the need for high accuracy solutions, a FEM code has been used following the formulation presented

```
function kc=getKcFromHalfFilledCavity (a ,b, c ,h, epr, sigmaCond, m,n, TEFlag, axisLimits ,
   resolution)

  kc = 0;

   syms kcsquared kcsym

   lhsEquation = sqrt(kcsym^2−(m*pi/a)^2−(n*pi/b)^2)*...
       cot(sqrt(kcsym^2−(m*pi/a)^2−(n*pi/b)^2)*(c−h ));
   eprMod = epr − 1 i *sigmaCond*4*pi*1e−7*299792458/kcsym ;
   rhsEquation = −sqrt(eprMod*kcsym^2−(m*pi/a)^2−(n*pi/b)^2)*...
       cot(sqrt(eprMod*kcsym^2−(m*pi/a)^2−(n*pi/b)^2)*h );

   if (nargin > 10)
     digitsOld = digits ( resolution );
     equation = lhsEquation−rhsEquation == 0;
    kc = vpasolve (equation, kcsym, axisLimits);
    digits(digitsOld);
   else
      close all
       fplot(real(lhsEquation),axisLimits)
       hold on
       fplot (real(rhsEquation),axisLimits);
       fplot (imag(rhsEquation),axisLimits);
  end
```

FIGURE 5 Code used in Section 3.3

```
function [ kc , indices ]=getAllKcFromCircCavity (a ,h,numKc, resolution )

  if (nargin == 3)
  resolution = 16;

  end

  digitsOld = digits ( resolution );

  kc = sym(zeros (1 , 2*numKc^3)); indices = zeros (4, 2*numKc^3);

  counter = 1;

  for m = 0:numKc
    for n = 1:numKc
      for  p  =  0:numKc
       if (p>0) % TE mode
           kc( counter ) = sqrt (( getZerosBesselFunction . . .
             (m,n, true , resolution )/a)^2+(p*pi/h)^2); indices (: , counter ) =
           [m, n, p, −1];
           counter = counter + 1;
        end
        % TM mode
        kc( counter ) = sqrt (( getZerosBesselFunction . . .
           (m,n, false , resolution )/a)^2+(p*pi/h)^2); indices (: , counter ) =
        [m, n, p, −2];
        counter = counter + 1;
      end
    end
  end

  % To remove zeros.

  indices = indices (: ,1: counter −1);
  kc = kc (: ,1: counter −1);

  [ kc , sorted_indices ] = sort(kc );

  indices = indices (: , sorted_indices );

  kc = kc (1:numKc);
  indices = indices (: ,1:numKc);
  digits ( digitsOld )
```

FIGURE 6 Code used in Section 3.4

```
function zeroValue = getZerosBesselFunction (m,n, isDer , resolution )

if (nargin <= 3)
resolution = 16;

end

syms z
if ( isDer )
equation=besselj (m−1,z)−besselj (m+1,z) == 0;
else
equation=besselj (m, z) == 0;
end
digitsOld = digits ( resolution );
zeroValue=vpasolve ( equation , z , getGuess (m,n, isDer ));
digits ( digitsOld );
```

FIGURE 7 Code used in Figure 6

TABLE 1 Analytical and FEM results for Section 3.1

Mode	k_0, anal (m^{-1})	k_0, FEM (m^{-1})
TM_{110}	523.5987755982989	523.5987755954994
TM_{101}	702.4814731040726	702.4814731055401
TM_{011}	755.1448932759318	755.1448932818443
TM_{210}	755.1448932759318	755.1448933141208

Abbreviations: FEM, finite element method; TM, transversal magnetic mode.

TABLE 2 Analytical and FEM results for Section 3.2

Mode	k_0, anal (m^{-1})	k_0, FEM (m^{-1})
TEz_{101}	353.7837746270816	353.7837746271084
TEz_{201}	544.5048974571262	544.5048974588835
TEz_{102}	599.7987417164069	599.7987417192613
TEz_{301}	750.3144561169121	750.3144561537357

Abbreviations: FEM, finite element method; TE, transversal electric mode.

TABLE 3 Analytical and FEM results for Section 3.3

Mode	k_0, anal (m^{-1})	k_0, FEM (m^{-1})
TEz_{101}	137.8767675996847+ 80.99383192059738i	137.8767676507687+ 80.9938318794768i
TEz_{201}	225.1186934508449+ 86.94553938560484i	225.1186946175216+ 86.9455389264532i
TEz_{011}	247.8733488761241+ 88.02137628504226i	247.8733494478111+ 88.0213763074423i
TEz_{111}	267.3250562043701+ 88.79947416219282i	267.3250567462096+ 88.7994741360851i

Abbreviations: FEM, finite element method; TE, transversal electric mode.

TABLE 4 Analytical and FEM results for Section 3.4

Mode	k_0, anal (m^{-1})	k_0, FEM (m^{-1})
TEz_{101}	2.404825557695773	2.404825558023451
TEz_{201}	3.831705970207512	3.831705986521815
TEz_{102}	5.135622301840683	5.135622426682891
TEz_{301}	5.520078110286311	5.520078419608677

Abbreviations: FEM, finite element method; TE, transversal electric mode.

in Section 2. Also, for convenience, the code has been uploaded in Reference 28. The discretization is introduced through triangular prisms due to the characteristics of all the cavities presented in this communication (which can be meshed through structured meshes). The mesher used is gmsh,[29] since it provides high-order curved meshes for simplices. The procedure followed in this paper is, first, generate a 2D mesh with triangles and, then, extrude that mesh in the structured direction. The solver used to get the solution from the system of equations is a direct LU solver in order not to have any error due to the use of iterative solvers. Also, the integration rules used are enough to get accurate to machine precision (in this case, double precision) results. The number of layers is chosen to have elements close to regular prisms. Basis functions for $p = 4$ from Reference 11 have been used, so results close to double precision are obtained. The eigenvalue sparse solver is the MATLAB implementation of ARPACK.[20]

For the rectangular cavity, the analytical results for the first four resonant modes with a resolution of 16 significant digits are included in Table 1 given $a = 0.01$ m, $b = 0.0075$ m, and $c = 0.005$ m. For the FEM solution, 356 876 unknowns for 3296 elements with an average edge length of 0.65 mm were necessary. It can be seen the high accuracy provided by the FEM code, which agrees with the analytical results.

The same results are shown in Table 2 for the half-filled cavity with geometrical parameters of $a = 0.01$ m, $b = 0.001$ m, $c = 0.01$ m, $h = 0.005$ m and $\varepsilon_r = 2$. Regarding the FEM simulation, 240 028 unknowns for 2100 elements with an average edge length of 0.48 mm were used.

With respect to the lossy cavity, $a = 0.02286$ m, $b = 0.02286$ m, $c = 0.01016$ m, $h = 0.01143$ m, $\varepsilon_r = 2$ and $\sigma = 1$S/m have been used. The analytical results and the FEM results are shown in Table 3, showing a good agreement. For the FEM simulation, 688 elements with an average length of 5.65 mm have been used, obtaining 154 344 unknowns.

Finally, a circular cavity with $\rho = 1$ m and $h = 0.5$ m has been simulated, showing in Table 4 the analytical values and the simulation results obtained from the FEM code. For this, a fourth-order geometric mesh has been generated with 516 elements, with an average length of 0.19 m, leading to a problem with 58 172 unknowns.

5 | CONCLUSIONS

In this communication, four different cavity problems ready to use as a testbench in the CEM community have been proposed. Details about the approach used to solve the problem and the formulation used for a FEM code have been presented. Also, mathematical codes based on a symbolic toolbox have been included, providing arbitrary accuracy useful for high accuracy codes (such as high order FEM). Finally, different examples have been given and the accuracy of the results has been shown with a FEM code with fourth-order basis functions.

ORCID

Adrian Amor-Martin https://orcid.org/0000-0002-6123-4324

REFERENCES

1. MacKie-Mason B, Shao Y, Greenwood A, Peng Z. Supercomputingenabled first-principles analysis of radio wave propagation in urban environments. *IEEE Trans Antennas Propag*. 2018;66(12):6606-6617.
2. Jin J-M, Yan S. Multiphysics modeling in electromagnetics: technical challenges and potential solutions. *IEEE Antennas Propag Mag*. 2019;61(2):14-26.
3. Garcia-Donoro D, Garcia-Castillo LE, Ting SW. Verification process of finite-element method code for electromagnetics: using the method of manufactured solutions. *IEEE Antennas Propag Mag*. April 2016;58(2):28-38.
4. Amor-Martin A, Garcia-Castillo LE. Construction of higher-order curl-conforming finite elements and its assembly. *Int J RF Microw Comput-aided Eng*. 2019;29(8):e21753.
5. Marsic N, Geuzaine C. Efficient finite element assembly of high order Whitney forms. Paper presented at: 9th IET International Conference on Computation in Electromagnetics (CEM 2014); London, United Kingdom; 2014.
6. Solov'ev S. Quadrature finite element method for elliptic eigenvalue problems. *Lobachevskii J Math*. 2017;38(5):856-863.
7. Beig DAO, Wang J, Peng Z, Lee J-F. A universal array approach for finite elements with continuously inhomogeneous material properties and curved boundaries. *IEEE Trans Antennas Propag*. 2012;60(10):4745-4756.
8. Ingelstrom P. A new set of h (curl)-conforming hierarchical basis functions for tetrahedral meshes. *IEEE Trans Microw Theory Tech*. 2006;54(1):106-114.
9. Amor-Martin A, Garcia-Castillo LE, Garcia-Doñoro DD. Secondorder Nédélec curl-conforming prismatic element for computational electromagnetics. *IEEE Trans Antennas Propag*. 2016;64(10):4384-4395.
10. Graglia RD, Wilton DR, Peterson AF. Higher order interpolatory vector bases for computational electromagnetics. *IEEE Trans Antennas Propag*. 1997;45(3):329-342.
11. Fuentes F, Keith B, Demkowicz L, Nagaraj S. Orientation embedded high order shape functions for the exact sequence elements of all shapes. *Comput Math Appl*. 2015;70(4):353-458.
12. Arndt D, Bangerth W, Davydov D, et al. The deal. ii library, version 8.5. *J Numer Math*. 2017;25(3):137-145.
13. Badia S, Martín AF, Principe J. Fempar: an object-oriented parallel finite element framework. *Archiv Comput Methods Eng*. 2018;25(2):195-271.
14. Gillette A, Kloefkorn T. Trimmed serendipity finite element differential forms. *Math Comput*. 2019;88(316):583-606.
15. Buffa A, Sangalli G, Vázquez R. Isogeometric analysis in electromagnetics: B-splines approximation. *Comput Methods Appl Mech Eng*. 2010;199(17–20):1143-1152.
16. C. Reddy, M. D. Deshpande, C. Cockrell, and F. B. Beck, "*Finite Element Method for Eigenvalue Problems in Electromagnetics*," 1994.
17. Chatterjee A, Jin J, Volakis J. Computation of cavity resonances using edge-based finite elements. *IEEE Trans Microw Theory Tech*. 1992;40(11):2106-2108.
18. Moghaddar A, Walton EK. Time-frequency distribution analysis of scattering from waveguide cavities. *IEEE Trans Antennas Propag*. 1993;41(5):677-680.
19. Lee J-H, Xiao T, Liu QH. A 3-d spectral-element method using mixed-order curl conforming vector basis functions for electromagnetic fields. *IEEE Trans Microw Theory Tech*. 2006;54(1):437-444.
20. Lehoucq RB, Sorensen DC, Yang C. *ARPACK Users' Guide: Solution of Large-Scale Eigenvalue Problems with Implicitly Restarted Arnoldi Methods*. Vol 6. SIAM; 1998.
21. Char BW, Geddes KO, Gonnet GH, Leong BL, Monagan MB, Watt S. *Maple V Library Reference Manual*. Springer Science & Business Media; 2013.
22. Wolfram S. The mathematica book. *Assembly Automation*; 1999.
23. *MATLAB version 9.3 (R2017b)*. Natick, MA: The Mathworks, Inc.; 2017.
24. F. Hivert and N. Thiéry, "*Mupad-Combinat, An Open-Source Package for Research in Algebraic Combinatorics*," 2004.
25. Accuracy of Bessel functions in MATLAB. https://www.advanpix.com/2016/05/12/accuracy-of-bessel-functions-in-matlab/. Accessed 2019–0909.
26. Monk P. *Finite Element Methods for Maxwell's Equations*. Oxford University Press; 2003.
27. Balanis CA. *Advanced Engineering Electromagnetics*. John Wiley & Sons; 1999.
28. A. Amor-Martin. aamorm/testbench: git repository for a testbench of arbitrary accuracy for electromagnetic simulations. June; 2020. https://doi.org/10.5281/zenodo.3885581
29. Geuzaine C, Remacle J-F. Gmsh: a 3-D finite element mesh generator with built-in pre-and post-processing facilities. *Int J Numer Methods Eng*. 2009;79(11):1309-1331.

AUTHOR BIOGRAPHY

Adrián Amor-Martín was born in Móstoles, Madrid, in 1989 and received a degree in Telecommunications Engineering in 2012, MSc in Multimedia and Communications in 2014, and the PhD in Multimedia and Communications in 2018 from the University Carlos III of Madrid. He participated as a researcher in the University Carlos III of Madrid from 2012 to 2018 with different scholarships obtained on a competitive basis. From 2019, he is a postdoc researcher at the Universität des Saarlandes, in Germany. He has authored nine publications in international journals and 16 contributions to international conferences. His research interests are focused on the

application of numerical methods to high-performance computational electromagnetics including finite elements, domain decomposition methods, the definition of basis functions, and hp adaptivity.

How to cite this article: Amor-Martin A. A testbench of arbitrary accuracy for electromagnetic simulations. *Int J RF Microw Comput Aided Eng*. 2020;30:e22342. https://doi.org/10.1002/mmce.22342